Proceedings of the Thirty-Fourth International Joint Conference on Artificial Intelligence (IJCAI-25)
Sister Conferences Best Papers Track

Scalable Graph Classification via Random Walk Fingerprints (Extended Abstract)*

Peiyan Li[1] , **Honglian Wang**[2] , **Christian Böhm**[3]
[1]LMU Munich, Germany
[2]KTH Royal Institute of Technology, Sweden
[3]University of Vienna, Austria
lipeiyan@dbs.ifi.lmu.de, honglian@kth.se, christian.boehm@univie.ac.at

Abstract

We design a lightweight structural feature extraction technique for graph classification. It leverages node subsets and connection strength reflected by random-walk-based heuristics, presenting a scalable, unsupervised, and easily interpretable alternative. We provide theoretical insights into our technical design and establish a relation between the extracted structural features and the graph spectrum. We show our method achieves high levels of computational efficiency while maintaining robust classification accuracy.

1 Introduction

We address the problem of graph classification. Similar to classifying text or image data, comparing graphs is fundamental to building a classifier. This task, known as graph similarity learning, is challenging due to the inherent variability in both the size and structure of the graphs.

Targeting graph similarity, the past decade has witnessed the success of graph kernels [Shervashidze *et al.*, 2011; Borgwardt and Kriegel, 2005] and graph representation learning [Kipf and Welling, 2017; Tsitsulin *et al.*, 2018]. The former compares substructures, while the latter utilizes supervised graph neural networks, or uses unsupervised embedding approaches paired with classifiers. Despite their success, scalability remains a critical issue. This is due to the increasing size of real-world graphs and the large volume of graph datasets, as both the scale of each graph and the number of graphs can be substantial. To address the scalability challenge, we introduce **R**andom **W**alk **F**ingerprints (RWF), an unsupervised structural feature extraction technique that can incorporate node attributes. The computational complexity of RWF is bounded by $\mathcal{O}(N\tau_c(mn + pn^2))$, where N is the number of graphs; n and m are the number of nodes and edges per graph; τ_c is the maximum walk steps; and p is the dimension of node features. In the worst-case scenario where $m = n^2$, RWF exhibits a cubic time complexity regarding n. However, the typical sparsity of real-world graphs ($m \ll n^2$) generally ensures more manageable computational demands.

[1]This is an extended abstract of a paper first published in the IEEE ICDM conference [Li *et al.*, 2024].

2 Method

At its core, RWF quantifies intra- and inter-subset connection strengths among node subsets with distinct structural roles. By focusing on these role-based subsets, RWF enables soft alignment between structurally heterogeneous graphs, enabling meaningful comparisons. Based on these node subsets, heuristics like loop and walk, reflecting the connection strength, are used to construct the feature vector. Additionally, RWF can easily incorporate node features. After feature extraction, we use a basic classifier like SVM to get the classification results.

Structural-Role-based Vertex Partitioning

We divide the nodes of each graph into distinct subsets, thereby facilitating alignment among the node subsets across disparate graphs. This essential step enables us to identify local graph patterns, thus enhancing the representation power of our method. Given a graph G, we partition its nodes into k subsets, i.e., $V = V_1 \cup \cdots \cup V_k$, where each subset contains nodes that share the same structural role, and k is the number of predefined roles. In order to obtain size-invariant representations of graphs, the parameter k should be consistent for all graphs.

- **Degree Heuristic.** Degree is an essential statistic of nodes. High-degree nodes tend to be cores in the local central regions, while low-degree nodes often occupy peripheral positions. Hence, node degree serves as a naive indicator of the structural roles of nodes. Initially, we count the node degrees. We then sort the nodes by their degrees and divide the node set into k subsets, each containing $|V|/k$ nodes.
- **Core-Periphery Heuristic.** This heuristic is based on the assumption that the arrangement of a graph includes densely connected core nodes and sparsely connected peripheral nodes. We utilize KM-config [Kojaku and Masuda, 2018] to identify core and peripheral nodes. It leverages the configuration model [Fosdick *et al.*, 2018] as the null model to generate a target graph with idealized core-periphery pairs. Then, it maximizes the similarity between the target and source graphs through appropriate node labeling. Notably, KM-config can detect multiple core-periphery pairs, and it has a linear time complexity with respect to the number of edges.

Structural Feature Extraction

With the node partitions of each graph determined, subsequently, we show how to extract features based on the graph G and its node partitions $(V_1, V_2, \cdots, V_k)$. In the simplest form, we quantify the connection strength within and between the subsets of nodes based on the relational matrix $\mathbf{T}$ and its powers. The relational matrix $\mathbf{T}$ can be defined by the transition matrix $\mathbf{T}_p = \mathbf{D}^{-1}\mathbf{A}$, or the symmetric normalized adjacency matrix $\mathbf{T} = \mathbf{D}^{-\frac{1}{2}}\mathbf{A}\mathbf{D}^{-\frac{1}{2}}$, where $\mathbf{D}$ denotes the diagonal degree matrix and $\mathbf{A}$ denotes the adjacency matrix. Each entry of $\mathbf{T}_p$ and $\mathbf{T}$ quantifies a kind of connection strength between two nodes. In this paper, we select $\mathbf{T}$ since symmetric normalization enables computational efficiency. We introduce the following features.

$$\texttt{loop}^{\tau}_{V_i} = \frac{1}{|V_i|}\sum_{v\in V_i}\mathbf{T}^{\tau}_{vv} \tag{1}$$

$$\texttt{walk}^{\tau}_{V_i} = \frac{1}{|V_i|^2}\sum_{u,v\in V_i}\mathbf{T}^{\tau}_{uv} \tag{2}$$

$$\texttt{walk}^{\tau}_{V_i\to V_j} = \frac{1}{|V_i|\times|V_j|}\sum_{u\in V_i, v\in V_j}\mathbf{T}^{\tau}_{uv} \tag{3}$$

Here, $\texttt{loop}^{\tau}_{V_i}$ represents the average strength of all $\tau-$loops of nodes in V_i. $\texttt{walk}^{\tau}_{V_i}$ represents the average strength of all $\tau-$walks that start and end at nodes within V_i. $\texttt{walk}^{\tau}_{V_i\to V_j}$ denotes the average strength of all $\tau-$walks traversing from V_i to V_j. In a nutshell, the three features measure the connection strength within and between node subsets.

Incorporation of Node Attributes

In addition to the structural features, our method is designed to incorporate node features. Accordingly, we define the following two matrices:

$$\mathbf{P} = \frac{1}{|V_i|}\mathbf{X}_{V_i}\cdot diag(\mathbf{T}^{\tau}_{V_i})\cdot\mathbf{X}^T_{V_i} \tag{4}$$

$$\mathbf{Q} = \frac{1}{|V_i|^2}\mathbf{X}_{V_i}\cdot\mathbf{T}^{\tau}_{V_i}\cdot\mathbf{X}^T_{V_i} \tag{5}$$

where $\mathbf{P}\in\mathbb{R}^{p\times p}$ and $\mathbf{Q}\in\mathbb{R}^{p\times p}$ are symmetric matrices encapsulating the interactions of node features within the node set V_i. Here, $diag(\mathbf{T}^{\tau}_{V_i})$ and $\mathbf{T}^{\tau}_{V_i}$ serve as kernels to modulate the influence of node features, while $\frac{1}{|V_i|}$ and $\frac{1}{|V_i|^2}$ are used to balance the numerical values. We further compute the row average of $\mathbf{P}$ and $\mathbf{Q}$, producing two vectors $\texttt{xl}^{\tau}_{V_i}\in\mathbb{R}^p$ and $\texttt{xw}^{\tau}_{V_i}\in\mathbb{R}^p$, which represent the aggregated features of the subset V_i at scale τ. This procedure yields a rich feature vector for the node subset that combines sub-structural and node-feature-based information.

3 Feature Interpretation

We demonstrate the connections between the extracted features and the graph spectrum, providing insight into the use of local feature extraction and a limited walking length.

Connections to Graph Spectrum

We factorize $\mathbf{T}$ as follows:

$$\mathbf{T} = \mathbf{U}\mathbf{\Lambda}\mathbf{U}^T \tag{6}$$

where the columns of $\mathbf{U}\in\mathbb{R}^{n\times n}$ are eigenvectors of $\mathbf{T}$, and $\mathbf{\Lambda}$ is the diagonal matrix whose diagonal elements are the corresponding eigenvalues, denoted by $\{\mathbf{\Lambda}_1,\cdots,\mathbf{\Lambda}_n\}$. Let $\mathbf{U}_{V_i}\in\mathbb{R}^{|V_i|\times n}$ be the rows of $\mathbf{U}$ that corresponds to V_i, specifically, we use the node indices of V_i to extract a subset of rows of $\mathbf{U}$ to form $\mathbf{U}_{V_i}$.

Let $\mathbf{B} = \mathbf{U}^T_{V_i}\mathbf{U}_{V_i}$, which is a symmetric $n\times n$ matrix, and $\{\alpha_1,\alpha_2,\cdots,\alpha_n\}$ are the corresponding diagonal entries. Let $\beta = \{\beta_1,\cdots,\beta_n\}\in\mathbb{R}^{1\times n}$ and $\gamma = \{\gamma_1,\cdots,\gamma_n\}\in\mathbb{R}^{1\times n}$ be the row vector with the sum over each column of $\mathbf{U}_{V_i}$ and $\mathbf{U}_{V_j}$, respectively. We have:

$$\texttt{loop}^{\tau}_{V_i} = \frac{1}{|V_i|}\sum_{t=1}^{n}\alpha_t\mathbf{\Lambda}^{\tau}_t \tag{7}$$

$$\texttt{walk}^{\tau}_{V_i} = \frac{1}{|V_i|^2}\sum_{t=1}^{n}\beta^2_t\mathbf{\Lambda}^{\tau}_t \tag{8}$$

$$\texttt{walk}^{\tau}_{V_i\to V_j} = \frac{1}{|V_i|\times|V_j|}\sum_{t=1}^{n}\beta_t\gamma_t\mathbf{\Lambda}^{\tau}_t \tag{9}$$

The above calculations establish the relationship between the three feature sets and the spectrum of $\mathbf{T}^{\tau}$, i.e., the three features represent the weighted aggregation of the eigenvalues of $\mathbf{T}^{\tau}$. Thus, the extracted features could be conceptualized as ensembles that capture the essence of the full eigenvalue spectrum of the graph. This connection may elucidate the efficacy of the extracted features, as several studies (e.g., [Tsitsulin *et al.*, 2018; Dong *et al.*, 2019; Sawlani *et al.*, 2021]) have demonstrated the effectiveness of graph spectrum in graph classification tasks.

Why Use Local Feature Extraction?

Consider $\mathbf{A}$ as the adjacency matrix of an undirected graph. We alter an arbitrary edge e_{uv} by adjusting its weight, and the updated adjacency matrix becomes $\hat{\mathbf{A}}$. After applying symmetric normalization to $\mathbf{A}$ and $\hat{\mathbf{A}}$, we get $\mathbf{T}$ and $\hat{\mathbf{T}}$, which denote the initial and modified transition matrices, respectively. We use $d(x,y)$ to represent the shortest path distance between two nodes x and y. For the perturbed edge uv, we introduce a distance function $\overline{d}(w) = \min\{d(w,u), d(w,v)\}$, which measures the minimum distance from any node w to either node in the pair u or v. We give the following theorem derived from [Pan *et al.*, 2022]. We have a different setting regarding $\mathbf{T}$ but the proof is the same.

Theorem 1. *Let* $V^{\tau} = \{x\in V, \overline{d}(x) > \tau\}$, *then* $\mathbf{T}^{\tau}_{xy} = \hat{\mathbf{T}}^{\tau}_{xy}$ *for all* $x, y\in V^{\tau}$. *[Proof omitted]*

Based on the above theorem, it is easy to understand that under structural perturbation, the change in $\mathbf{T}$ propagates outward from the perturbed nodes to their increasingly distant neighbors as the number of walk steps increases. If we omit the vertex partitioning process and only use $\texttt{loop}^{\tau}_{V}$ and $\texttt{walk}^{\tau}_{V}$ as features, we can still distinguish $\mathbf{A}$ and $\hat{\mathbf{A}}$. But with vertex partitioning and the three features defined, it is

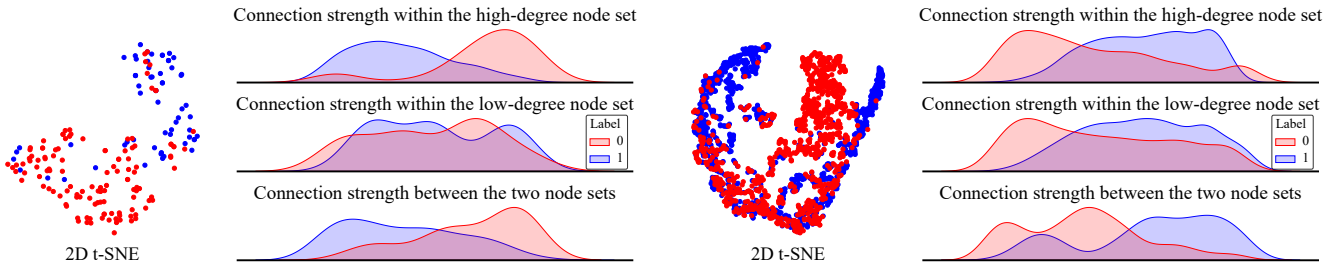

(a) MUTAG (b) REDDIT-BINARY

Figure 1: Visualization of Graph Structural Features Extracted by RWF. MUTAG and REDDIT-BINARY are two graph datasets, each containing multiple graphs. We derive a d-dimensional feature vector for each graph, which can be partitioned into three domains reflecting three kinds of connectivity patterns: intra-connectivity within high-degree nodes (d_1), intra-connectivity within low-degree nodes (d_2), and inter-connectivity between high-degree and low-degree nodes (d_3). The d-dimensional feature vectors from all the graphs are projected to 2-dimensional space for visualization using t-SNE, as (a) left and (b) left show. Additionally, the features of each graph from each domain (i.e., d_1, d_2, or d_3) are separately projected into 1-dimensional space using t-SNE. The density of these 1D projections is then estimated and illustrated in (a) right and (b) right.

possible to detect where the perturbation occurs, as node subsets act as local sensors. Therefore, vertex partitioning may enhance the distinguishing power of the defined features.

Fig. 1 shows the results of RWF on two graph datasets. Recall that the underlying assumption behind RWF is that graphs from different classes exhibit distinct local connectivity patterns. These patterns are reflected by node subsets that assume different structural roles. In the simplest form, we categorize the nodes of each graph into two subsets: high-degree and low-degree. Then we fix the maximum walk step τ_c to 6 and calculate $\{\texttt{loop}^{\tau}_{V_{high}}, \texttt{walk}^{\tau}_{V_{high}}\}^{\tau_c}_{\tau=1}$, $\{\texttt{loop}^{\tau}_{V_{low}}, \texttt{walk}^{\tau}_{V_{low}}\}^{\tau_c}_{\tau=1}$ and $\{\texttt{walk}_{V_{high}\to V_{low}}\}^{\tau_c}_{\tau=1}$. This division gives rise to three distinct feature domains: the connectivity strength within high-degree nodes, within low-degree nodes, and between high-degree and low-degree nodes. As illustrated in Fig. 1, RWF features demonstrate strong discriminatory capabilities. Moreover, we can observe distinctions between the distributions of different classes, even when considering a single domain of RWF features independently.

Why Limit Walk Steps?

We explain why we use a limited number of steps as controlled by τ_c. Due to the symmetric normalization, the eigenvalues of $\mathbf{T}$ are bounded within the interval $[-1, 1]$. Based on the above calculations, it is evident that the three features can be expressed as weighted aggregations of the eigenvalues of $\mathbf{T}^{\tau}$, like $f(\tau) = \sum_{t=1}^{n} \delta_t \mathbf{\Lambda}_t^{\tau}$, where the vector $\delta = \{\delta_1, \cdots, \delta_n\} \in \mathbb{R}^{1\times n}$ contains some constant values. Without loss of generality, we assume the eigenvalues are sorted in descending order, with Λ_1 and Λ_n representing the maximum and minimum eigenvalues, respectively. The maximum eigenvalue $\Lambda_1 = 1$. The minimum eigenvalue $\Lambda_n = -1$ if and only if the corresponding graph is bipartite; otherwise, Λ_n lies in the range of $(-1, 0]$. For simplicity, we assume Λ_n follows the latter case, as bipartite graphs are special, and we consider general cases here. When τ becomes large:

$$\lim_{\tau\to\infty} f(\tau) = \delta_1 \tag{10}$$

The above calculation reveals that $f(\tau) \approx \delta_1$ when τ is large, and δ_1 is a constant. This suggests that larger τ_c does not contribute additional structural information. In practice, we set τ_c to a value typically not exceeding 10 to ensure efficiency while capturing meaningful graph structure.

4 Experimental Evaluation

We evaluate our method against the following techniques:

- Unsupervised graph embedding algorithms: NetLSD [Tsitsulin *et al.*, 2018], NetSimile [Berlingerio *et al.*, 2013], FGSD [Verma and Zhang, 2017], A-DOGE [Sawlani *et al.*, 2021], LDP [Cai and Wang, 2018] and FEATHER [Rozemberczki and Sarkar, 2020].

	DEE	RED-12K	GIT	TWI
NetLSD	56.1	38.5	64.6	68.6
A-DOGE	55.6	<u>47.8</u>	67.0	69.5
FGSD	56.2	33.2	60.7	64.2
NetSimile	55.6	47.3	<u>68.8</u>	70.5
FEATHER	55.7	47.2	69.0	70.0
LDP	55.6	46.8	67.2	68.5
NH	56.0	‡	60.2	‡
WL	55.6	39.5	62.6	‡
DOSGK	55.7	‡	66.3	‡
GCN	56.8	45.9	61.3	69.0
GraphSAGE	56.8	42.2	53.7	61.4
GIN	<u>56.9</u>	47.3	61.4	68.7
RWF-CP	**57.1**	43.6	66.7	69.6
RWF-CP-feature	56.6	46.2	**70.4**	69.1
RWF-D	56.5	44.8	68.1	<u>71.3</u>
RWF-D-feature	55.9	**48.1**	**70.4**	**71.4**

Table 1: Mean graph classification accuracy (in %). Best results are marked in **bold**, and second bests are <u>underlined</u>. The mark "‡" refers to out of resources, indicating exhaustion of either time (> 24 hours) or memory.

- Graph kernels: NH [Hido and Kashima, 2009], WL [Shervashidze *et al.*, 2011], and DOSGK [Huang *et al.*, 2021].
- Graph neural networks: GCN [Kipf and Welling, 2017], GIN [Xu *et al.*, 2019], and GraphSAGE [Hamilton *et al.*, 2017].

Due to brevity, we only show the results on four large datasets. The reader can find all the experiments in [Li *et al.*, 2024].

The graph classification results on Deezer_ego_nets (DEE), REDDIT-MULTI-12K (RED-12K), Github_stargazers (GIT), and Twitch_egos (TWI), are reported in Table 1. RWFs achieve the best results in general.

5 Conclusion

In this paper, we proposed RWF, a scalable, interpretable, unsupervised feature extraction approach for graph classification. RWF learns a subset-based representation of graphs, central to which is the structural-role-based vertex partitioning scheme. This technique enables soft alignments across diverse graphs and thus facilitates the learning of local structures. Specifically, RWF extracts three features, measuring the connection strengths within and between node subsets. Additionally, a highlight of RWF is its flexibility in incorporating node attributes, making it a comprehensive tool for feature extraction. Our experimental analysis confirms the effectiveness and efficiency of RWF, illustrating its potential as a powerful approach to graph classification.

References

[Berlingerio *et al.*, 2013] Michele Berlingerio, Danai Koutra, Tina Eliassi-Rad, and Christos Faloutsos. Network similarity via multiple social theories. In *ASONAM*, pages 1439–1440, 2013.

[Borgwardt and Kriegel, 2005] Karsten M Borgwardt and Hans-Peter Kriegel. Shortest-path kernels on graphs. In *IEEE ICDM*, 2005.

[Cai and Wang, 2018] Chen Cai and Yusu Wang. A simple yet effective baseline for non-attribute graph classification. *ICLR workshops*, 2018.

[Dong *et al.*, 2019] Kun Dong, Austin R Benson, and David Bindel. Network density of states. In *ACM SIGKDD*, pages 1152–1161, 2019.

[Errica *et al.*, 2020] Federico Errica, Marco Podda, Davide Bacciu, and Alessio Micheli. A fair comparison of graph neural networks for graph classification. In *ICLR*, 2020.

[Feragen *et al.*, 2013] Aasa Feragen, Niklas Kasenburg, Jens Petersen, Marleen de Bruijne, and Karsten Borgwardt. Scalable kernels for graphs with continuous attributes. *NeurIPS*, 26, 2013.

[Fosdick *et al.*, 2018] Bailey K Fosdick, Daniel B Larremore, Joel Nishimura, and Johan Ugander. Configuring random graph models with fixed degree sequences. *SIAM Review*, pages 315–355, 2018.

[Hamilton *et al.*, 2017] Will Hamilton, Zhitao Ying, and Jure Leskovec. Inductive representation learning on large graphs. *NeurIPS*, 2017.

[Hido and Kashima, 2009] Shohei Hido and Hisashi Kashima. A linear-time graph kernel. In *IEEE ICDM*, pages 179–188, 2009.

[Huang *et al.*, 2021] Leo Huang, Andrew J Graven, and David Bindel. Density of states graph kernels. In *SDM*, pages 289–297. SIAM, 2021.

[Kipf and Welling, 2017] Thomas N. Kipf and Max Welling. Semi-supervised classification with graph convolutional networks. In *ICLR*, 2017.

[Kojaku and Masuda, 2018] Sadamori Kojaku and Naoki Masuda. Core-periphery structure requires something else in the network. *New Journal of physics*, 20(4):043012, 2018.

[Li *et al.*, 2024] Peiyan Li, Honglian Wang, and Christian Böhm. Scalable graph classification via random walk fingerprints. In *2024 IEEE International Conference on Data Mining (ICDM)*, pages 231–240. IEEE, 2024.

[Pan *et al.*, 2022] Liming Pan, Cheng Shi, and Ivan Dokmanić. Neural link prediction with walk pooling. In *ICLR*, 2022.

[Rozemberczki and Sarkar, 2020] Benedek Rozemberczki and Rik Sarkar. Characteristic functions on graphs: Birds of a feather, from statistical descriptors to parametric models. In *Proceedings of the 29th ACM international conference on information & knowledge management*, pages 1325–1334, 2020.

[Rozemberczki *et al.*, 2020] Benedek Rozemberczki, Oliver Kiss, and Rik Sarkar. Karate Club: An API Oriented Open-source Python Framework for Unsupervised Learning on Graphs. In *CIKM*, page 3125–3132, 2020.

[Sawlani *et al.*, 2021] Saurabh Sawlani, Lingxiao Zhao, and Leman Akoglu. Fast attributed graph embedding via density of states. In *IEEE ICDM*, pages 559–568, 2021.

[Shervashidze *et al.*, 2011] Nino Shervashidze, Pascal Schweitzer, Erik Jan Van Leeuwen, Kurt Mehlhorn, and Karsten M Borgwardt. Weisfeiler-lehman graph kernels. *JMLR*, 12(9), 2011.

[Tsitsulin *et al.*, 2018] Anton Tsitsulin, Davide Mottin, Panagiotis Karras, Alexander Bronstein, and Emmanuel Müller. Netlsd: hearing the shape of a graph. In *ACM SIGKDD*, pages 2347–2356, 2018.

[Verma and Zhang, 2017] Saurabh Verma and Zhi-Li Zhang. Hunt for the unique, stable, sparse and fast feature learning on graphs. *NeurIPS*, 2017.

[Vishwanathan *et al.*, 2010] S Vichy N Vishwanathan, Nicol N Schraudolph, Risi Kondor, and Karsten M Borgwardt. Graph kernels. *JMLR*, 11:1201–1242, 2010.

[Xu *et al.*, 2019] Keyulu Xu, Weihua Hu, Jure Leskovec, and Stefanie Jegelka. How powerful are graph neural networks? In *ICLR*, 2019.